to the non-uniformity of the CNT arrays within the platform as discussed in previous paragraphs. This study revealed the preferred positions of the substrates in terms of uniform growth length. The obtained knowledge could apply to future scale up of CNT arrays manufacturing by CVD.

Acknowledgements

This work was partly supported by NSF grants CMMI-0727250 and Dr. Shaochen Chen, CMS-0510823 and Dr. Shih-Chi Liu, NCA&T the Center for Advanced Materials and Smart Structures (NSF Grant #0205803), and DURIP-Office of Naval Research.

REFERENCES

[1] Yun Y, Shanov V, Tu Y, Subramaniam S, Schulz MJ. Growth mechanism of long aligned multiwall carbon nanotube arrays by water-assisted chemical vapor deposition. J Phys Chem B 2006;110(47):23920–5.
[2] Schulz MJ, Kelkar AD, Sundaresan MJ. Nanoengineering of structural, functional, and smart materials. CRC Press; 2006.
[3] Yasuda S, Futaba DN, Yumura M, Iijima S, Hata K. Diagnostics and growth control of single-walled carbon nanotube forests using a telecentric optical system for in situ height monitoring. Appl Phys Lett 2008;93(14):143115-1–3.
[4] Chen T-T, Liu Y-M, Sung Y, Wang H-T, Ger M-D. Experimental investigation on carbon nanotube grown by thermal chemical vapor deposition using non-isothermal deposited catalysts. Mater Chem Phys 2006;97:511–6.
[5] de los Arcos T, Garnier MG, Seo JW, Oelhafen P, Thommen V, Mathys D. The influence of catalyst chemical state and morphology on carbon nanotube growth. J Phys Chem B 2004;108(23):7728–34.
[6] Chakrabarti S, Kume H, Pan L, Nagasaka T, Nakayama Y. Number of walls controlled synthesis of millimeter-long vertically aligned brushlike carbon nanotubes. J Phys Chem C 2007;111:1929–34.
[7] Kukovitsky EF, L'vov SG, Sainov NA, Shustov VA, Chernozatonskii LA. Correlation between metal catalyst particle size and carbon nanotube growth. Chem Phys Lett 2002;355:497–503.
[8] Futaba DN, Hata K, Yamada T, Mizuno K, Yumura M, Iijima S. Kinetics of water-assisted single-walled carbon nanotube synthesis revealed by a time-evolution analysis. Phys Rev Lett 2005;95:056104.
[9] Li XS, Zhang XF, Ci LJ, Shah R, Wolfe C, Kar S, et al. Air-assisted growth of ultra-long carbon nanotube bundles. Nanotechnology 2008;19(45):455609.
[10] Patole SP, Alegaonkar PS, Lee HC, Yoo JB. Optimization of water assisted chemical vapor deposition parameters for super growth of carbon nanotubes. Carbon 2008;46(14):1987–93.
[11] Bronikowski MJ. CVD growth of carbon nanotube bundle arrays. Carbon 2006;44(13):2822–32.
[12] Jeong GH, Olofsson N, Falk LKL, Campbell EEB. Effect of catalyst pattern geometry on the growth of vertically aligned carbon nanotube arrays. Carbon 2009;47(3):696–704.
[13] Li G, Chakrabarti S, Schulz M, Shanov V. Growth of aligned multi-walled carbon nanotubes on bulk copper substrates by CVD. J Mater Res 2009;24(9):2813–20.

Fabrication of porous SiC_y (core)/C (shell) fibres using a hybrid precursor of polycarbosilane and pitch

Zengyong Chu [a,], Rongan He [a], Xiaobin Zhang [b], Zheng Jiang [c], Haifeng Cheng [a], Yingde Wang [a], Xiaodong Li [a]*

[a] *Key Laboratory of New Ceramic Fibres & Composites, National University of Defence Technology, Changsha 410073, China*
[b] *Advanced Science Research Laboratory, Saitama Institute of Technology, 1690 Fusaiji, Fukaya, Saitama 369-0293, Japan*
[c] *Inorganic Chemistry Laboratory, Department of Chemistry, University of Oxford, OX1 3QR, UK*

ARTICLE INFO

Article history:
Received 3 November 2009
Accepted 31 January 2010
Available online 4 February 2010

ABSTRACT

Porous SiC_y (core)/C (shell) composite fibres have been fabricated using a simple KOH controlled-activation of SiC_x fibres, which were pyrolyzed from polycarbosilane-pitch blend fibres. Effects of activation conditions and pyrolysis temperatures were studied. There are distinctive interfaces observed on the cross-sections of the co-axial fibres, where Si content varies gradually from the core to the shell. The etching of Si follows a slow "core-reducing" process in N_2, while in CO_2, cracks are frequently observed on the shells due to the accelerated activations. V-shaped Si-free carbon fibres could be obtained when a lower pyrolysis temperature was used to produce the SiC_x fibres.

* *Corresponding author:* Fax: +86 731 84573165.
E-mail address: chuzy@nudt.edu.cn (Z. Chu).
0008-6223/$ - see front matter © 2010 Elsevier Ltd. All rights reserved.
doi:10.1016/j.carbon.2010.01.064

Microporous carbon (MC)-based materials have received intensive attention in the context of physisorption for hydrogen storage in the coming era of hydrogen economy [1]. Recently, tremendous efforts have been made to prepare MCs with high specific surface areas (SSAs) and developed porosity, typically, high SSAs can be achieved by controlled-activation of carbon precursors [3], template-assembling using Zeolites [2], or metal-extracting from carbides (carbide-derived carbons, CDCs) [4]. All these candidates have shown brilliant future for the hydrogen storage. However, the amounts of hydrogen adsorbed are still quite limited under high pressure and ambient temperature conditions [5]. Fortunately, the modification of C surfaces through incorporation of functional groups or dopants facilitates increasing binding energy of hydrogen with MCs and most recently, B-substituted MC has been synthesized and exhibited increased H_2 storage capacity, 3.2 wt.%, almost double that of MC with similar SSA [6]. As simulated [7], Si should be a good alternative dopant due to the much higher binding energy of hydrogen with SiC. However, SiC usually has low SSA and hard to fabricate porous structure. We here reported a simple one-step activation to produce porous SiC fibres using a hybrid precursor of polycarbosilane (PCS) and pitch. Interestingly, novel core–shell structured materials were obtained. The influences of processing parameters on the cross-section morphologies were discussed in this letter.

Polycarbosilane and pitch were mixed with a weight ratio of 55%/45%, melt-spun into green fibres, cured in air and pyrolyzed in N_2 giving C-rich SiC_x fibres. Then the SiC_x fibres were loaded with KOH at a definite impregnation mass ratio ($R = wt.\ KOH/wt.\ fibres$), and activated in N_2 or CO_2 at a defined temperature/duration (for experimental details, see Supplementary information).

Fig. 1 shows the scanning electron microscope (SEM) images of typical activated fibres derived from precursor fibres pyrolyzed at 1200 °C. Co-axial characteristics of the fibres can be clearly observed in Fig. 1(a)–(c). There are distinctive interfaces between the cores and the shells. However, a big difference, as shown in Fig. 1(d), can be found on those activated fibres from 800 °C-pyrolyzed ones. Their cross-sections are V-shaped. This is a result of the high activation weight loss, 74.5 wt.%. This morphology has not been observed on general activated carbon fibres, despite that their activation weight loss can amount to 80 wt.% [8]. The sample (d) is nearly Si-free, with a total pore volume and a SSA increased to 0.80 $m^3\ g^{-1}$ and 975 $m^2\ g^{-1}$, respectively. The pure MC fibres with V-shaped cross-sections can be prepared by deliberate control of the pyrolysis and activation conditions. The results indicate that the mild pyrolysis temperature of the precursor fibres favours the removal of Si in the subsequent KOH activation.

A "core-reducing" process can be observed as the activation time goes on from 1 h in Fig. 1(a) to 3 h in Fig. 1(b). The "core-reducing" process is formed because the distribution of KOH is not uniform. It is understandable that the concentration of KOH is very high at the surface because molten KOH is infiltrated from the surface. More importantly, its reaction rate with SiC is lower than that with C. The thickness of the shells increases from ~2 to ~4 μm as the KOH activation duration extends. Their SSAs are 962 and 1116 $m^2\ g^{-1}$ respectively. The increase of the SSA indicates the shell is porous. But the SSAs are not proportional to the thickness of the shells, implying that both the shell and the core have become porous during the early activation, for example, in Fig. 1(a). This is reasonable because the present inorganic fibres are C-rich, with the starting carbon content approaching to 61 wt.%. At the beginning, C could be activated through out the whole fibres, as can be seen from the K distribution in Fig. 2(a), characterised using the energy dispersive X-ray spectroscopy (EDS) axial line-scanning on the cross-section of the

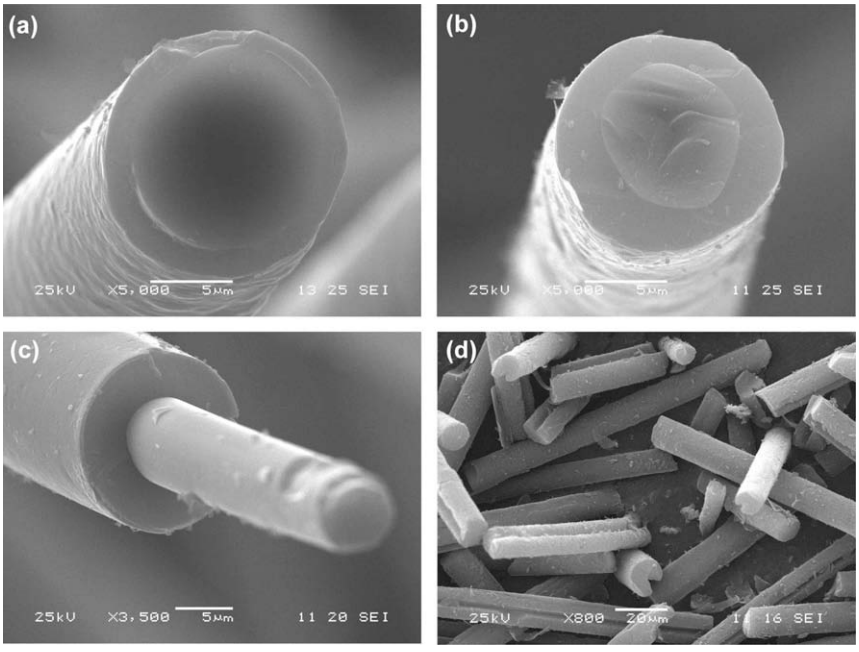

Fig. 1 – SEM images of typical activated fibres.

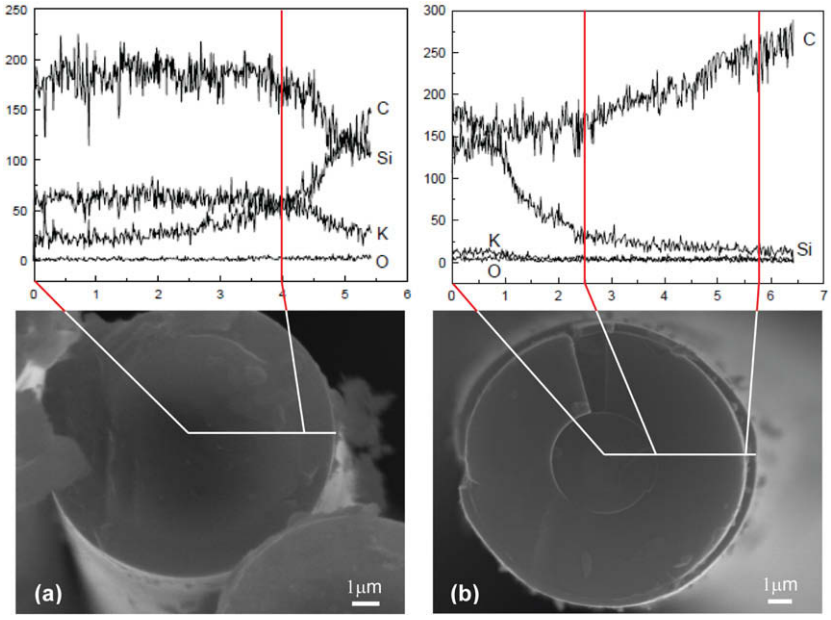

Fig. 2 – EDS line-scanning on the cross-section of activated fibres.

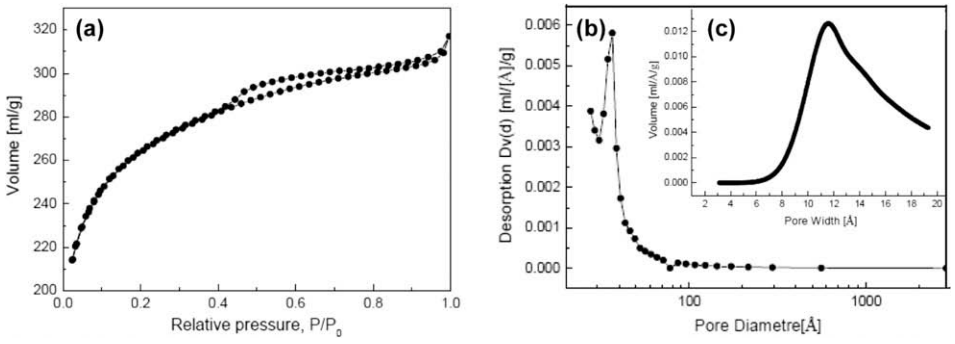

Fig. 3 – (a) N_2 adsorption and desorption isotherms of activated fibres in Fig. 2(a) and corresponding (b) mesopore and (c) micropore size distribution curves calculated from the adsorption isotherm by the BJH and HK methods respectively.

fibres. The existence of K in the core indicates the penetration of KOH to the core. So, it is possible that some micropores were introduced in the core, even though their volume is probably lower than that near the surface. It also indicates that more KOH introduced at the beginning, more micropores could be introduced throughout the whole fibres. This was confirmed by the great effect of the impregnation ratio, whose increasing from 1.0 to 1.5–2.4 leads to an immediate increasing of the SSA from 230–490 to 960–1250 $m^2\ g^{-1}$. XRD results have shown that all the samples are in an amorphous state.

Besides the impregnation ratio, the activation atmosphere also plays an important role because they can be a combination of physical activation (*e.g.*, CO_2) and chemical activation (KOH). As shown in Fig. 2(b), most Si was removed from the shell when activated in CO_2. It shows a screw-like end surface with the thickness of the shell larger than 4 μm. In the case of activation in N_2, Fig. 2(a), Si was largely retained despite the higher impregnation ratio, 2.4 (in N_2) *vs.* 1.5 (in CO_2). This is because the oxidative CO_2 could accelerate the activation of SiC [8]. In CO_2, both C and SiC were activated very quickly, to the extent that cracks were frequently observed on the shells. At the end of the activated fibres, the shell may partially split off the core, resulting in a core-protruding morphology, as shown in Fig. 1(c).

Chen et al. [9] reported the formation of core–shell structures when making CDCs from SiC whiskers but only the shell is porous. In our case, both the core and the shell of the fibres are porous, in which Si is still remained in the core. This is a result of the faster activation rate of C than SiC under selected conditions, in other words, relatively slow etching rate of Si to C.

In this study, the sample in Fig. 2(a) has the highest SSA, 1025 $m^2\ g^{-1}$, with a total pore volume and an average pore size of 0.49 $cm^3\ g^{-1}$ and 1.98 nm respectively. Its N_2 adsorption and desorption isotherms are shown in Fig. 3(a), which exhibit a type IV behaviour with hysteresis, indicating the existence of mesopores in the fibres. The pore size distributions of mesopores and micropores are shown in Fig. 3(b) and (c), whose average diameters are 3.65 and 1.16 nm, respectively, as calculated from the adsorption branch using the Barrett–Joyner–Halenda (BJH) and the Horvath–Kawazoe

(HK) methods. Further studies are needed to control the pore size distributions for specific applications, for example, increasing micropore volume for hydrogen storage.

In summary, using SiC_x fibres derived from the pyrolysis of the hybrid precursor fibres of PCS and pitch, a proper control of the activation conditions can yield the co-axial porous composite fibres with high SSA. The porosity and component of the activated fibres may be adjusted by facile control the activation conditions. This kind of core–shell structured fibres can be regarded as Si-substituted activated carbon fibres, which may be promising functional materials, for example, as potential hydrogen storage materials and catalyst supports. This approach can also be adopted for the preparation of M-substituted activated carbon fibres if M-containing polymers (or blends) are used as the starting material.

Acknowledgement

The authors gratefully acknowledge financial support of National Natural Science Foundation of China (No. 50403010).

Appendix A. Supplementary data

Supplementary data associated with this article can be found, in the online version, at doi:10.1016/j.carbon.2010.01.064.

REFERENCES

[1] Mandal TK, Gregory DH. Hydrogen storage materials: present scenarios and future directions. Annu Rep Prog Chem Sect A 2009;105:21–54.
[2] Lee J, Kim J, Hyeon T. Recent progress in the synthesis of porous carbon materials. Adv Mater 2006;18(16):2073–9.
[3] Wang HL, Gao QM, Hu J. High hydrogen storage capacity of porous carbons prepared by using activated carbon. J Am Chem Soc 2009;131(20):7016–22.
[4] Gogotsi Y, Welz S, Ersoy DA, McNallan MJ. Conversion of silicon carbide to crystalline diamond-structured carbon at ambient pressure. Nature (London) 2001;411(6835):283–7.
[5] Thomas KM. Adsorption and desorption of hydrogen on metal – organic framework materials for storage applications: comparison with other nanoporous materials. Dalton Trans 2009;9:1487–505.
[6] Chung TCM, Jeong Y, Chen Q, Kleinhammes A, Wu Y. Synthesis of microporous boron-substituted carbon (B/C) materials using polymeric precursors for hydrogen physisorption. J Am Chem Soc 2008;130(21):6668–9.
[7] Mpourmpakis G, Froudakis GE, Lithoxoos GP, Samios J. SiC nanotubes: a novel material for hydrogen storage. Nano Lett 2006;6(8):1581–3.
[8] Macia-Agullo JA, Moore BC, Cazorla-Amoros D, Linares-Solano A. Activation of coal tar pitch carbon fibres: physical activation vs. chemical activation. Carbon 2004;42(7):1367–70.
[9] Chen XQ, Cantrell DR, Kohlhaas K, Stankovich S, Ibers JA, Jaroniec M, et al. Carbide-derived nanoporous carbon and novel core–shell nanowires. Chem Mater 2006;18(3):753–8.

Microwave assisted exfoliation and reduction of graphite oxide for ultracapacitors

Yanwu Zhu, Shanthi Murali, Meryl D. Stoller, Aruna Velamakanni, Richard D. Piner, Rodney S. Ruoff *

Department of Mechanical Engineering and the Texas Materials Institute, The University of Texas at Austin, One University Station C2200, Austin, TX 78712-0292, USA

ARTICLE INFO

Article history:
Received 20 October 2009
Accepted 1 February 2010
Available online 4 February 2010

ABSTRACT

We report a simple yet versatile method to simultaneously achieve the exfoliation and reduction of graphite oxide. By treating graphite oxide powders in a commercial microwave oven, reduced graphite oxide materials could be readily obtained within 1 min. Extensive characterizations showed that the as-prepared materials consisted of crumpled, few-layer thick and electronically conductive graphitic sheets. Using the microwave exfoliated graphite oxide as electrode material in an ultracapacitor cell, specific capacitance values as high as 191 F/g have been demonstrated with KOH electrolyte.

* *Corresponding author.*
E-mail address: r.ruoff@mail.utexas.edu (R.S. Ruoff).
0008-6223/$ - see front matter © 2010 Elsevier Ltd. All rights reserved.
doi:10.1016/j.carbon.2010.02.001